2009-03-16

Second-Order Structural Analysis with One Element per Member

Jesse William Lyon
Brigham Young University - Provo

SECOND-ORDER STRUCTURAL ANALYSIS WITH ONE ELEMENT PER MEMBER

by

Jesse W. Lyon

A thesis submitted to the faculty of

Brigham Young University

in partial fulfillment of the requirements for the degree of

Master of Science

Department of Civil and Environmental Engineering

Brigham Young University

April 2009

BRIGHAM YOUNG UNIVERSITY

GRADUATE COMMITTEE APPROVAL

of a thesis submitted by

Jesse W. Lyon

This thesis has been read by each member of the following graduate committee and by majority vote has been found to be satisfactory.

Date	Richard J. Balling, Chair
Date	David W. Jensen, Member
Date	Paul W. Richards, Member

BRIGHAM YOUNG UNIVERSITY

As chair of the candidate's graduate committee, I have read the thesis of Jesse W. Lyon in its final form and have found that (1) its format, citations, and bibliographical style are consistent and acceptable and fulfill university and department style requirements; (2) its illustrative materials including figures, tables, and charts are in place; and (3) the final manuscript is satisfactory to the graduate committee and is ready for submission to the university library.

Date

Richard J. Balling
Chair, Graduate Committee

Accepted for the Department

E. James Nelson
Graduate Coordinator

Accepted for the College

Alan R. Parkinson
Dean, Ira A. Fulton College of Engineering and Technology

ABSTRACT

SECOND-ORDER STRUCTURAL ANALYSIS WITH ONE ELEMENT PER MEMBER

Jesse W. Lyon

Department of Civil and Environmental Engineering

Master of Science

In this thesis, formulas for the local tangent stiffness matrix of a plane frame member are derived by differentiating the member resistance vector in the displaced position. This approach facilitates an analysis using only one element per member. The formulas are checked by finite difference. The derivation leads to the familiar elastic and geometric stiffness matrices used by other authors plus an additional higher order geometric stiffness matrix.

Contributions of each of the three sub-matrices to the tangent stiffness matrix are studied on both the member and structure levels through two numerical examples. These same examples are analyzed three different ways for comparison. First, the examples are analyzed using the method presented in this thesis. Second, they are analyzed with the finite element modeling software ABAQUS/CAE using only one element per member. Third, they are analyzed with ABAQUS using 200 elements per member. Comparisons

are made assuming the ABAQUS analysis which uses 200 elements per member is the most accurate. The element presented in this thesis performs much better than the ABAQUS analysis which uses one element per member, with maximum errors of 1.0% and 40.8% respectively, for a cantilever column example. The maximum error for the two story frame example using the ABAQUS analysis with one element per member is 42.8%, while the results from the analysis using the element presented in this thesis are within 1.5%. Using the element presented in this thesis with only one element per member gives good and computationally efficient results for second-order analysis.

ACKNOWLEDGMENTS

The work presented in this thesis has resulted from the efforts of several individuals. I would like to acknowledge my advisor, Dr. Richard J. Balling, for his previous work on this subject, his encouragement and suggestions. I would also like to thank my committee members for their time and effort in assisting me in this work. Finally, I would like to thank my wife, Kristi, for her constant love and support, which enabled me to complete this thesis.

TABLE OF CONTENTS

LIST OF TABLES

LIST OF FIGURES

1 Introduction

The first objective of this thesis is to present a second-order nonlinear plane frame analysis method which uses only one element per member. Many of the procedures currently available employ finite element techniques which involve dividing the members of the frame into multiple elements for a more accurate analysis. Analyzing large frames with such an approach can be computationally intensive. The analysis presented herein uses a single element per member.

The finite element modeling software ABAQUS/CAE is used to illustrate the importance of this objective in Section 4 of this thesis. The results from ABAQUS models using only one element per member are compared to the results of ABAQUS models which use 200 elements per member. The resulting joint displacements are very different, with errors as large as 41% for a cantilever column example and 43% for a two-story plane frame example.

The second objective is to derive a tangent stiffness matrix for the plane frame element that is the direct derivative of the resistance vector. This relationship stems from the Newton-Raphson method used in the nonlinear matrix stiffness method. To illustrate the importance of this direct derivation, a brief summary of the Newton-Raphson method follows.

For a second-order analysis, the governing equation of the matrix stiffness method is shown in Equation 1-1.

$$f = z(u) \tag{1-1}$$

where f is the force vector of the element, and z is known as the resistance vector, a nonlinear function of the displacement vector u. To solve this system of nonlinear equations, an iterative solution method is used, namely the Newton-Raphson method (Cheney and Kincaid 2008). The procedure begins with an initial guess for u,

$$u^{(0)} = (u_1^{(0)}, u_2^{(0)}, u_3^{(0)}, ..., u_i^{(0)})^T \tag{1-2}$$

which is an approximate solution to Equation 1-1. Let Δu be a correction vector for the initial displacement vector, $u^{(0)}$, such that

$$\begin{aligned} u^{(0)} + \Delta u = (&u_1^{(0)} + \Delta u_1, u_2^{(0)} + \Delta u_2, u_3^{(0)} \\ &+ \Delta u_3, ..., u_i^{(0)} + \Delta u_i)^T \end{aligned} \tag{1-3}$$

is a more accurate solution. The Taylor expansion leads to the following equation

$$f \approx z(u^{(0)} + \Delta u) \approx z(u^{(0)}) + k_T \Delta u \tag{1-4}$$

where k_T is the Jacobian matrix, which in structural analysis is the tangent stiffness matrix. It is defined by

$$k_T = z'(u^{(0)}) = \begin{bmatrix} \frac{\partial z_1}{\partial u_1} & \frac{\partial z_1}{\partial u_2} & \frac{\partial z_1}{\partial u_3} & \cdots & \frac{\partial z_1}{\partial u_i} \\ \frac{\partial z_2}{\partial u_1} & \frac{\partial z_2}{\partial u_2} & \frac{\partial z_2}{\partial u_3} & & \\ \frac{\partial z_3}{\partial u_1} & \frac{\partial z_3}{\partial u_2} & \frac{\partial z_3}{\partial u_3} & & \\ \vdots & & & \ddots & \\ \frac{\partial z_i}{\partial u_1} & & & & \frac{\partial z_i}{\partial u_i} \end{bmatrix} \tag{1-5}$$

Note that the tangent stiffness matrix is the derivative of the resistance vector with respect to each of the displacements. If k_T is nonsingular, then the corrected displacements can be found by solving Equation 1-4 for Δu.

The derivation of the tangent stiffness matrix presented in section 3 of this thesis is the work of Dr. Richard J. Balling. The remainder of this thesis, including an extensive literature review in Section 2, the analysis of two examples in Section 4 and their comparisons to ABAQUS analyses, the validation of the derivation of the tangent stiffness matrix by finite difference and the study of the contributions of the three sub-matrices to the tangent stiffness matrix is the work of Jesse W. Lyon.

2 Literature Review

In the literature, a variety of methods exist for the derivation of the element tangent stiffness matrix. However, many of these methods are not sufficiently accurate for the analysis of long slender members without the use of multiple elements. Also, a majority of these tangent stiffness matrices are not derived from the relationship between the resistance vector and the tangent stiffness matrix.

Typically, the tangent stiffness matrix is the sum of two matrices, the elastic and geometric stiffness matrices. The elastic stiffness matrix accounts for the effects of the elastic deformations of the element, and is generally the same throughout the literature. The geometric stiffness matrix deals with the effects of large displacements on the element, and varies depending on the derivation.

The conventional method of deriving the tangent stiffness matrix uses the principle of virtual work or virtual displacements, and the general or simplified beam theory equations are presented in Yang and Kuo (1994). While analyzing curved beams, Yang et al. (2007) summarized the conventional method. Their derivation of the stiffness matrix for a two-dimensional beam element is applicable to this thesis. The incremental equilibrium for the response of an element to externally applied loads is derived from the principle of virtual work. Then using the finite element procedure, an incremental stiffness equation for the element is obtained, which includes both the elastic and

geometric stiffness matrices. This approach has also been employed by Yang and Chiou (1987), Zhao and Wong (2006), and Leu et al. (2008).

Yang and McGuire (1986) presented a similar derivation. They modified the incremental stiffness equation by including a nonuniform torsional force in the element force vector. This leads to a more complex tangent stiffness matrix.

Yang et al. (2002) developed the elastic and geometric stiffness matrices from force-displacement relationships derived using incremental theory. The deformation of a beam element due to externally applied loads is described as being a series of small incremental translations and rotations. These displacements are calculated for each step with reference to the previous step; however, rigid body motion is excluded. After deriving the element forces and moments, the elastic and geometric stiffness matrices are calculated. This procedure produces a tangent stiffness matrix that is identical to the conventional stiffness matrix presented by Yang and Kuo (1994).

Izzudin (2006) used a rotational spring analogy to determine the geometric stiffness of both a two-dimensional and three-dimensional frame element. The stiffness of a beam element is related to the stiffness of a rotational spring attached to the element and the element chord. The stiffness of the spring is calculated using simple linear kinematics, which leads to a linear tangent stiffness matrix. This method is conceptually easy to understand and can be modified such that only a single member is required for a simplified linear analysis. This approach does not produce a tangent stiffness matrix that is the direct derivative of the element resistance vector.

Oran (1973a) proposed a derivation of the tangent stiffness matrix using a differential relationship between the stiffness matrix and the element force vector similar

to the one used in the Newton-Raphson method. The member force vector presented by Oran (1973a) differs from the member resistance vector used in this thesis in that it contains only three elements instead of six elements. As a result, Oran's member tangent stiffness matrix is a 3x3 elastic stiffness matrix. Oran (1973b) extended the previous derivation to three dimensions. Chandra et al. (1990) used the same geometric stiffness matrix as Oran (1973b) in their analysis method.

Gu and Chan (2000) derived the stiffness matrix of an element which included the effects of initial imperfections. The equations of equilibrium which incorporate the imperfections are constructed for the element in its deformed configuration. Force-deflection equations are then derived from the equilibrium equations, and the tangent stiffness matrix of the element is computed using a derivative approach similar to Oran (1973a). The analysis they presented requires only one element per member. Gu and Chan (2005) extended this derivation to space frames.

The inclusion of initial imperfections in the derivation was also explored by Chan and Zhou (1995). The deformed shape of the member is assumed to be a fifth-order polynomial. Boundary conditions are applied that incorporate the initial imperfection in order to obtain the shape function for the element, which is used to derive the energy function. The tangent stiffness matrix is formed by a differential equation involving the total potential energy function. Once again, this approach does not take advantage of the relationship between the resistance vector and the tangent stiffness matrix.

Albermani and Kitipornchai (1990) presented a tangent stiffness matrix that was comprised of a deformation stiffness matrix in addition to the conventional elastic and geometric stiffness matrices. An equation for the strain energy in terms of the axial strain

is derived using the principle of virtual displacements. Using a Lagrange interpolation polynomial to approximate the displacement field, the strain energy equation is integrated over the cross sectional area of the element. The resulting equation includes the deformation stiffness matrix, which is a function of the element deformations.

Zhou and Chan (2004a) derived the secant and tangent stiffness matrices which incorporate the formation of a plastic hinge along the length of the element. A displacement function is derived as the superposition of an elastic deformation function and a triangular plastic deformation function. Then, using the total potential energy function modified to account for the plastic hinges, the member forces are developed. The tangent stiffness matrix is derived by differentiating the force vector with respect to the member displacements, similar to Oran (1973a). Zhou and Chan (2004b) extended this derivation to incorporate three plastic hinges per member. The formation of plastic hinges allows an analysis that uses only a single element per member.

Haktanir (1994) developed a tangent stiffness matrix for planar bars using force-displacement relationships and the method of complementary functions. Equations for the stiffness of the element, along with the constitutive and compatibility equations are used to derive a set of governing differential equations for the behavior of the element. These equations are used to calculate the member end forces. From the equation relating the member displacements to the member end forces, the element tangent stiffness matrix is derived by the method of complementary functions.

Moran et al. (1998) proposed a derivation of the secant and tangent stiffness matrices using strain energy. First, the total strain energy is calculated by integrating the function for the strain energy density within the element volume. An equation for the

total potential energy is obtained by using the principle of virtual work. Then, by employing the finite element procedure, symmetric expressions for the generalized and simplified secant and tangent stiffness matrices are derived.

So and Chan (1991) presented a tangent stiffness matrix for a modified Hermite cubic beam element. First, a shape function for the element is derived using the assumption that the deflected shape of the element is a fourth-order polynomial. Then, from the total potential energy function of the element, the tangent stiffness matrix is calculated.

The element derived in this thesis allows for an analysis using only a single element per member. The tangent stiffness matrix for this element is the direct derivative of the resistance vector, and as such can be incorporated directly into the Newton-Raphson method. In order to achieve the objectives of this thesis, certain simplifications were made in the derivation of the tangent stiffness matrix. For example, the governing constitutive equation for the second-order Euler beam theory used is

$$M = EI\frac{d\theta}{dx}$$

where the derivative of the slope is with respect to the local coordinate axis, x which runs longitudinally along the undeformed member. Shoup and McLarnan (1971) presented a more accurate equation with reference to the arc length of the element in the deformed configuration, as follows

$$M = EI\frac{d\theta}{ds}$$

Though this equation leads to a more complicated solution to the differential equations within the analysis, it deserves future investigation.

3 Derivation of the Member Tangent Stiffness Matrix

The member tangent stiffness matrix is the direct derivative of the member resistance vector with respect to the member displacements. In this chapter a formula for the member resistance vector as a function of the member displacements will first be derived. The derivation of the member tangent stiffness matrix, involving the differentiation of the resistance vector will follow.

3.1 The Member Resistance Vector

The member resistance vector is the set of forces required to hold the member in a displaced position. Consider the single plane frame member shown in Figure 3-1. The dashed line represents the deformed configuration of the member.

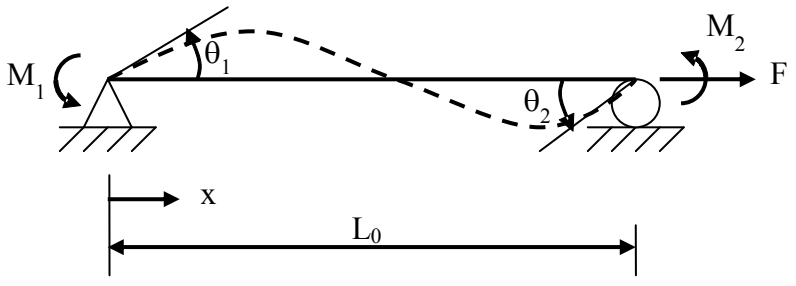

Figure 3-1 A Plane Frame Member

Expressions for the member end moments, M_1 and M_2 are obtained using the governing differential equation of second-order Euler beam theory,

$$EI\frac{d^4\Delta}{dx^4} - F\frac{d^2\Delta}{dx^2} = 0 \qquad \textbf{(3-1)}$$

where E is the modulus of elasticity of the member, I is the moment of inertia of the cross section, F is the axial force in the member and Δ is the equation for the deformed configuration of the member in terms of x. The solution to Equation 3-1 can be written in terms of the nodal rotations, θ_1 and θ_2,

$$\begin{aligned} \mathrm{M}_1 &= \left(\frac{4\mathrm{EI}}{\mathrm{L}_0} + \mathrm{FL}_0\mathrm{A}_\mathrm{G}\right)\theta_1 + \left(\frac{2\mathrm{EI}}{\mathrm{L}_0} + \mathrm{FL}_0\mathrm{B}_\mathrm{G}\right)\theta_2 \\ \mathrm{M}_2 &= \left(\frac{2\mathrm{EI}}{\mathrm{L}_0} + \mathrm{FL}_0\mathrm{B}_\mathrm{G}\right)\theta_1 + \left(\frac{4\mathrm{EI}}{\mathrm{L}_0} + \mathrm{FL}_0\mathrm{C}_\mathrm{G}\right)\theta_2 \end{aligned} \qquad \textbf{(3-2)}$$

where L_0 is the undeformed length of the member. For a more thorough derivation of Equation 3-2 refer to Appendix A. A_G, B_G and C_G are the geometric coefficients and are dependent on the sign of the axial force. For $F < 0$

$$\begin{aligned} A_G = C_G &= -\frac{\sin\lambda - \lambda\cos\lambda}{\lambda(2 - 2\cos\lambda - \lambda\sin\lambda)} + \frac{4}{\lambda^2} \\ B_G &= -\frac{\lambda - \sin\lambda}{\lambda(2 - 2\cos\lambda - \lambda\sin\lambda)} + \frac{2}{\lambda^2} \end{aligned} \qquad \textbf{(3-3)}$$

where

$$\lambda = L_0\sqrt{\frac{-F}{EI}}$$

If $F > 0$, the geometric coefficients are

$$A_G = C_G = \frac{\lambda\cosh\lambda - \sinh\lambda}{\lambda(2 - 2\cosh\lambda - \lambda\sinh\lambda)} - \frac{4}{\lambda^2}$$
$$B_G = -\frac{\sin\lambda - \lambda}{\lambda(2 - 2\cosh\lambda - \lambda\sinh\lambda)} - \frac{2}{\lambda^2} \qquad \textbf{(3-4)}$$

where

$$\lambda = L_0\sqrt{\frac{F}{EI}}$$

As λ goes to zero, both Equations 3-3 and 3-4 degenerate to

$$A_G = C_G = \frac{2}{15} \qquad B_G = -\frac{1}{30} \qquad \textbf{(3-5)}$$

The rotation angles θ_1 and θ_2 in Equation 3-2 can also be written in terms of the member displacements with the use of Figure 3-2, which shows the geometric properties of a plane frame member for both the original and deformed positions.

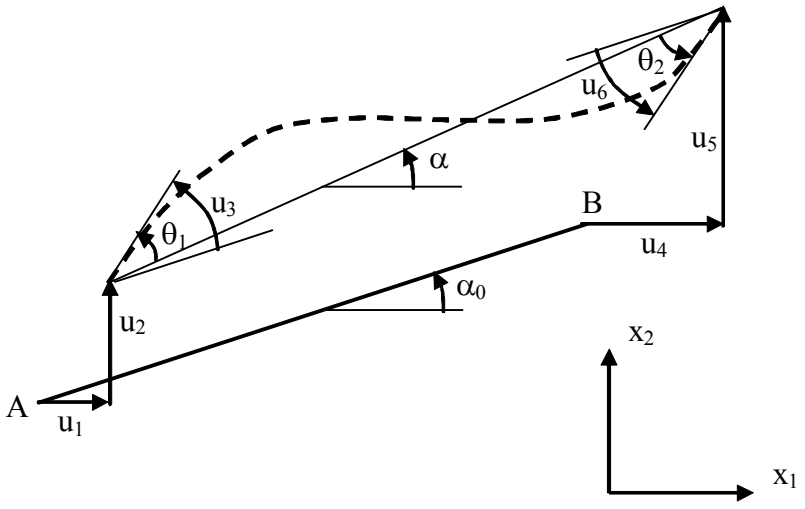

Figure 3-2 Geometric Properties of a Plane Frame Member

The member in its deformed position is represented by the dashed line. The initial position of the member is represented by the solid straight line between points A and B. The coordinates of A and B in the global coordinate system are (x_1^A, x_2^A) and (x_1^B, x_2^B), respectively. Note that translational displacements u_1 and u_4 are parallel to the global x_1 axis, and translational displacements u_2 and u_5 are parallel to the global x_2 axis. Note that rotational displacements u_3 and u_6 are measured from lines parallel to the initial line between A and B, while rotations θ_1 and θ_2 are measured from a straight line between the displaced ends of the member. The original length of the member is given by the following equation

$$L_0 = \sqrt{(x_1^B - x_1^A)^2 + (x_2^B - x_2^A)^2} \quad \textbf{(3-6)}$$

The deformed length of the member due to the nodal translations is defined as follows

$$L = \sqrt{(x_1^B + u_4 - x_1^A - u_1)^2 + (x_2^B + u_5 - x_2^A - u_2)^2} \quad \textbf{(3-7)}$$

The nodal rotations measured from the deformed reference line are

$$\theta_1 = u_3 - (\alpha - \alpha_0) \text{ and } \theta_2 = u_6 - (\alpha - \alpha_0) \quad \textbf{(3-8)}$$

where

$$\alpha = \sin^{-1}\left(\frac{x_2^B + u_5 - x_2^A - u_2}{L}\right) \text{ and } \alpha_0 = \sin^{-1}\left(\frac{x_2^B - x_2^A}{L_0}\right) \quad \textbf{(3-9)}$$

The axial force, F is given by the following equation

$$F = \frac{EA}{L_0}\left(L - L_0\right) \tag{3-10}$$

Using simple statics, the member resistance vector can then be written as

$$\hat{z} = \begin{bmatrix} -F \\ \frac{\left(M_1 + M_2\right)}{L} \\ M_1 \\ F \\ -\frac{\left(M_1 + M_2\right)}{L} \\ M_2 \end{bmatrix} \tag{3-11}$$

The ^ above z signifies that the end forces of magnitude F and $(M_1+M_2)/L$ in Equation 3-11 are parallel to the axes of the local member coordinate system. The local $\hat{x}_1$ axis runs from the displaced position of A to the displaced position of B, and the local $\hat{x}_2$ axis is normal to the local $\hat{x}_1$ axis. A transformation matrix is used to convert the member stiffness matrices and resistance vectors from the local coordinate system of each member to the global coordinate system, so that they are all compatible with one another. The orthogonal transformation matrix for plane frames is defined as follows

$$T = \begin{pmatrix} \cos\alpha & \sin\alpha & 0 & 0 & 0 & 0 \\ -\sin\alpha & \cos\alpha & 0 & 0 & 0 & 0 \\ 0 & 0 & 1 & 0 & 0 & 0 \\ 0 & 0 & 0 & \cos\alpha & \sin\alpha & 0 \\ 0 & 0 & 0 & -\sin\alpha & \cos\alpha & 0 \\ 0 & 0 & 0 & 0 & 0 & 1 \end{pmatrix} \tag{3-12}$$

where

$$\cos\alpha = \frac{x_1^B + u_4 - x_1^A - u_1}{L}$$
$$\sin\alpha = \frac{x_2^B + u_5 - x_2^A - u_2}{L} \qquad \textbf{(3-13)}$$

The global member resistance vector, written as a transformation of the local member resistance vector is

$$z = T\hat{z} \qquad \textbf{(3-14)}$$

3.2 Derivation of the Member Tangent Stiffness Matrix

The global member tangent stiffness matrix is the derivative of the global member resistance vector. However, for computation within the matrix stiffness method, the local tangent stiffness matrix is used. The local tangent stiffness matrix is written as

$$\hat{k}_T = Tk_T T^T \qquad \textbf{(3-15)}$$

Knowing the relationship between the global resistance vector and the global tangent stiffness matrix, and then substituting from Equation 3-14, Equation 3-15 becomes

$$\begin{aligned}\hat{k}_T &= T\left[\frac{\partial z}{\partial u_1} \quad \frac{\partial z}{\partial u_2} \quad \frac{\partial z}{\partial u_3} \quad \frac{\partial z}{\partial u_4} \quad \frac{\partial z}{\partial u_5} \quad \frac{\partial z}{\partial u_6}\right]T^T \\ &= T\left[\frac{\partial(T\hat{z})}{\partial u_1} \quad \frac{\partial(T\hat{z})}{\partial u_2} \quad \frac{\partial(T\hat{z})}{\partial u_3} \quad \frac{\partial(T\hat{z})}{\partial u_4} \quad \frac{\partial(T\hat{z})}{\partial u_5} \quad \frac{\partial(T\hat{z})}{\partial u_6}\right]T^T\end{aligned} \qquad \textbf{(3-16)}$$

Using the product rule, Equation 3-16 becomes

$$\hat{k}_T = T\left[\frac{\partial\left(T^T\right)}{\partial u_1}\hat{z} \quad \frac{\partial\left(T^T\right)}{\partial u_2}\hat{z} \quad \frac{\partial\left(T^T\right)}{\partial u_3}\hat{z} \quad \frac{\partial\left(T^T\right)}{\partial u_4}\hat{z} \quad \frac{\partial\left(T^T\right)}{\partial u_5}\hat{z} \quad \frac{\partial\left(T^T\right)}{\partial u_6}\hat{z}\right]T^T + \left[\frac{\partial\hat{z}}{\partial u_1} \quad \frac{\partial\hat{z}}{\partial u_2} \quad \frac{\partial\hat{z}}{\partial u_3} \quad \frac{\partial\hat{z}}{\partial u_4} \quad \frac{\partial\hat{z}}{\partial u_5} \quad \frac{\partial\hat{z}}{\partial u_6}\right]T^T \tag{3-17}$$

In order to continue with the derivation, a few preliminary steps are performed. First, the equation for the deformed length given in Equation 3-7 is differentiated with respect to the member displacements. The following 6 equations constitute Equation 3-18.

$$\begin{aligned}
\frac{\partial L}{\partial u_1} &= -\cos\alpha \\
\frac{\partial L}{\partial u_2} &= -\sin\alpha \\
\frac{\partial L}{\partial u_3} &= 0 \\
\frac{\partial L}{\partial u_4} &= \cos\alpha \\
\frac{\partial L}{\partial u_5} &= \sin\alpha \\
\frac{\partial L}{\partial u_6} &= 0
\end{aligned} \tag{3-18}$$

Second, the end rotations are differentiated with respect to each member displacement. To do this, α and α_0 are differentiated. Remember that the length, L, is a function of the member displacements, so the derivatives of α and α_0 involve the application of the chain rule.

The following 7 equations constitute Equations 3-19 and 3-20.

$$\frac{\partial \alpha}{\partial u_1} = \frac{\sin\alpha}{L}$$
$$\frac{\partial \alpha}{\partial u_2} = -\frac{\cos\alpha}{L}$$
$$\frac{\partial \alpha}{\partial u_3} = 0 \qquad \textbf{(3-19)}$$
$$\frac{\partial \alpha}{\partial u_4} = -\frac{\sin\alpha}{L}$$
$$\frac{\partial \alpha}{\partial u_5} = \frac{\cos\alpha}{L}$$
$$\frac{\partial \alpha}{\partial u_6} = 0$$

$$\frac{\partial \alpha_0}{\partial u_1} = \frac{\partial \alpha_0}{\partial u_2} = \frac{\partial \alpha_0}{\partial u_3} = \frac{\partial \alpha_0}{\partial u_4} = \frac{\partial \alpha_0}{\partial u_5} = \frac{\partial \alpha_0}{\partial u_6} = 0 \qquad \textbf{(3-20)}$$

The following derivatives of θ_1 and θ_2 constitute Equation 3-21.

$$\frac{\partial \theta_1}{\partial u_1} = \frac{\partial \theta_2}{\partial u_1} = -\frac{\partial \alpha}{\partial u_1} = -\frac{\sin\alpha}{L}$$
$$\frac{\partial \theta_1}{\partial u_2} = \frac{\partial \theta_2}{\partial u_2} = -\frac{\partial \alpha}{\partial u_2} = \frac{\cos\alpha}{L}$$
$$\frac{\partial \theta_1}{\partial u_3} = 1$$
$$\frac{\partial \theta_2}{\partial u_3} = 0 \qquad \textbf{(3-21)}$$
$$\frac{\partial \theta_1}{\partial u_4} = \frac{\partial \theta_2}{\partial u_4} = -\frac{\partial \alpha}{\partial u_4} = \frac{\sin\alpha}{L}$$
$$\frac{\partial \theta_1}{\partial u_5} = \frac{\partial \theta_2}{\partial u_5} = -\frac{\partial \alpha}{\partial u_5} = -\frac{\cos\alpha}{L}$$
$$\frac{\partial \theta_1}{\partial u_6} = 0$$
$$\frac{\partial \theta_2}{\partial u_6} = 1$$

Third, the cosine and sine of α must be differentiated with respect to the different displacements. The following equations constitute Equation 3-22.

$$\begin{aligned}
&\frac{\partial(\cos\alpha)}{\partial u_1} = -\frac{\sin^2\alpha}{L} \\
&\frac{\partial(\sin\alpha)}{\partial u_1} = \frac{\cos\alpha\sin\alpha}{L} \\
&\frac{\partial(\cos\alpha)}{\partial u2} = \frac{\cos\alpha\sin\alpha}{L} \\
&\frac{\partial(\sin\alpha)}{\partial u_2} = -\frac{\cos^2\alpha}{L} \\
&\frac{\partial(\cos\alpha)}{\partial u_3} = \frac{\partial(\sin\alpha)}{\partial u_3} = 0 \\
&\frac{\partial(\cos\alpha)}{\partial u_4} = \frac{\sin^2\alpha}{L} \\
&\frac{\partial(\sin\alpha)}{\partial u_4} = -\frac{\cos\alpha\sin\alpha}{L} \\
&\frac{\partial(\cos\alpha)}{\partial u_5} = -\frac{\cos\alpha\sin\alpha}{L} \\
&\frac{\partial(\sin\alpha)}{\partial u_5} = \frac{\cos^2\alpha}{L} \\
&\frac{\partial(\cos\alpha)}{\partial u_6} = \frac{\partial(\sin\alpha)}{\partial u_6} = 0
\end{aligned} \qquad \textbf{(3-22)}$$

The derivative of the transformation matrix with respect to u_1 can now be determined.

$$\frac{\partial T}{\partial u_1} = -\frac{\sin\alpha}{L}\begin{pmatrix}
\sin\alpha & -\cos\alpha & 0 & 0 & 0 & 0 \\
\cos\alpha & \sin\alpha & 0 & 0 & 0 & 0 \\
0 & 0 & 0 & 0 & 0 & 0 \\
0 & 0 & 0 & \sin\alpha & -\cos\alpha & 0 \\
0 & 0 & 0 & \cos\alpha & \sin\alpha & 0 \\
0 & 0 & 0 & 0 & 0 & 0
\end{pmatrix} = -S\frac{\sin\alpha}{L}$$

where

$$S = \begin{pmatrix} \sin\alpha & -\cos\alpha & 0 & 0 & 0 & 0 \\ \cos\alpha & \sin\alpha & 0 & 0 & 0 & 0 \\ 0 & 0 & 0 & 0 & 0 & 0 \\ 0 & 0 & 0 & \sin\alpha & -\cos\alpha & 0 \\ 0 & 0 & 0 & \cos\alpha & \sin\alpha & 0 \\ 0 & 0 & 0 & 0 & 0 & 0 \end{pmatrix}$$

The remaining derivatives of the transformation matrix are similarly derived. The preceding equation and the following 5 equations constitute Equation 3-23.

$$\begin{aligned} \frac{\partial T}{\partial u_2} &= S\frac{\cos\alpha}{L} \\ \frac{\partial T}{\partial u_3} &= 0 \\ \frac{\partial T}{\partial u_4} &= S\frac{\sin\alpha}{L} \\ \frac{\partial T}{\partial u_5} &= -S\frac{\cos\alpha}{L} \\ \frac{\partial T}{\partial u_6} &= 0 \end{aligned} \qquad \textbf{(3-23)}$$

Substituting from Equation 3-23, Equation 3-17 then becomes

$$\begin{aligned} \hat{k}_T &= \frac{1}{L}T\left[-\left(S^T\sin\alpha\right)\hat{z} \quad \left(S^T\cos\alpha\right)\hat{z} \quad 0 \quad \left(S^T\sin\alpha\right)\hat{z} \quad -\left(S^T\cos\alpha\right)\hat{z} \quad 0\right]T^T \\ &+\left[\frac{\partial\hat{z}}{\partial u_1} \quad \frac{\partial\hat{z}}{\partial u_2} \quad \frac{\partial\hat{z}}{\partial u_3} \quad \frac{\partial\hat{z}}{\partial u_4} \quad \frac{\partial\hat{z}}{\partial u_5} \quad \frac{\partial\hat{z}}{\partial u_6}\right]T^T \end{aligned}$$

$$\begin{aligned} \hat{k}_T &= \frac{1}{L}TS^T\hat{z}\left[-\sin\alpha \quad \cos\alpha \quad 0 \quad \sin\alpha \quad -\cos\alpha \quad 0\right]T^T \\ &+\left[\frac{\partial\hat{z}}{\partial u_1} \quad \frac{\partial\hat{z}}{\partial u_2} \quad \frac{\partial\hat{z}}{\partial u_3} \quad \frac{\partial\hat{z}}{\partial u_4} \quad \frac{\partial\hat{z}}{\partial u_5} \quad \frac{\partial\hat{z}}{\partial u_6}\right]T^T \end{aligned} \qquad \textbf{(3-24)}$$

After some matrix multiplication, Equation 3-24 becomes

$$\hat{k}_T = \frac{1}{L}\begin{bmatrix} \hat{z}_2 \\ -\hat{z}_1 \\ 0 \\ \hat{z}_5 \\ -\hat{z}_4 \\ 0 \end{bmatrix}\begin{bmatrix} 0 & 1 & 0 & 0 & -1 & 0 \end{bmatrix} + \begin{bmatrix} \frac{\partial \hat{z}}{\partial u_1} & \frac{\partial \hat{z}}{\partial u_2} & \frac{\partial \hat{z}}{\partial u_3} & \frac{\partial \hat{z}}{\partial u_4} & \frac{\partial \hat{z}}{\partial u_5} & \frac{\partial \hat{z}}{\partial u_6} \end{bmatrix} T^T$$

$$\hat{k}_T = \frac{1}{L}\begin{bmatrix} 0 & \hat{z}_2 & 0 & 0 & -\hat{z}_2 & 0 \\ 0 & -\hat{z}_1 & 0 & 0 & \hat{z}_1 & 0 \\ 0 & 0 & 0 & 0 & 0 & 0 \\ 0 & \hat{z}_5 & 0 & 0 & -\hat{z}_5 & 0 \\ 0 & -\hat{z}_4 & 0 & 0 & \hat{z}_4 & 0 \\ 0 & 0 & 0 & 0 & 0 & 0 \end{bmatrix} \quad \textbf{(3-25)}$$

$$+ \begin{bmatrix} \frac{\partial \hat{z}}{\partial u_1} & \frac{\partial \hat{z}}{\partial u_2} & \frac{\partial \hat{z}}{\partial u_3} & \frac{\partial \hat{z}}{\partial u_4} & \frac{\partial \hat{z}}{\partial u_5} & \frac{\partial \hat{z}}{\partial u_6} \end{bmatrix} T^T$$

The local member resistance vector give in Equation 3-11 must be differentiated with respect to each of the displacements, u_1 through u_6. Equation 3-11 is repeated below.

$$\hat{z} = \begin{bmatrix} -F \\ \frac{(M_1 + M_2)}{L} \\ M_1 \\ F \\ -\frac{(M_1 + M_2)}{L} \\ M_2 \end{bmatrix} \quad \textbf{(3-11)}$$

where M_1 and M_2 are given by Equation 3-2, and F is given by Equation 3-10. Each term in the resistance vector is dependent on some or all of the member displacements. The

equations for the end moments and axial force are substituted into Equation 3-11 and the geometric coefficients are assumed to be the constants given by Equation 3-5 in order to find the derivatives of the resistance vector. Equation 3-11 and its derivatives, along with Equation 3-12 are then substituted into Equation 3-25 and the local member tangent stiffness matrix is determined to be

$$\hat{k}_T = \hat{k}_E + \hat{k}_{G1} + \hat{k}_{G2} \tag{3-26}$$

where

$$\hat{k}_E = \frac{EI}{L_0}\begin{bmatrix} \frac{A}{I} & 0 & 0 & -\frac{A}{I} & 0 & 0 \\ 0 & \frac{12}{L^2} & \frac{6}{L} & 0 & -\frac{12}{L^2} & \frac{6}{L} \\ 0 & \frac{6}{L} & 4 & 0 & -\frac{6}{L} & 2 \\ -\frac{A}{I} & 0 & 0 & \frac{A}{I} & 0 & 0 \\ 0 & -\frac{12}{L^2} & -\frac{6}{L} & 0 & \frac{12}{L^2} & -\frac{6}{L} \\ 0 & \frac{6}{L} & 2 & 0 & -\frac{6}{L} & 4 \end{bmatrix} \tag{3-27}$$

$$\hat{k}_{G1} = FL_0\begin{bmatrix} 0 & 0 & 0 & 0 & 0 & 0 \\ 0 & \frac{1}{LL_0}+\frac{1}{5L^2} & \frac{1}{15L} & 0 & -\frac{1}{LL_0}-\frac{1}{5L^2} & \frac{1}{15L} \\ 0 & \frac{1}{15L} & \frac{2}{15} & 0 & -\frac{1}{15L} & -\frac{1}{30} \\ 0 & 0 & 0 & 0 & 0 & 0 \\ 0 & -\frac{1}{LL_0}-\frac{1}{5L^2} & -\frac{1}{15L} & 0 & \frac{1}{LL_0}+\frac{1}{5L^2} & -\frac{1}{15L} \\ 0 & \frac{1}{15L} & -\frac{1}{30} & 0 & -\frac{1}{15L} & \frac{2}{15} \end{bmatrix} \tag{3-28}$$

$$\hat{k}_{G2} = EA\begin{bmatrix} 0 & D_3 & 0 & 0 & -D_3 & 0 \\ D_3 - \dfrac{(D_1+D_2)}{L} & 0 & 0 & -D_3 + \dfrac{(D_1+D_2)}{L} & 0 & 0 \\ -D_1 & 0 & 0 & -D_1 & 0 & 0 \\ 0 & -D_3 & 0 & 0 & D_3 & 0 \\ -D_3 + \dfrac{(D_1+D_2)}{L} & 0 & 0 & 0 & 0 & 0 \\ D_2 & 0 & 0 & -D_2 & 0 & 0 \end{bmatrix} \quad \textbf{(3-29)}$$

where

$$D_1 = \frac{2\theta_1}{15} - \frac{\theta_2}{30} \qquad D_2 = \frac{2\theta_2}{15} - \frac{\theta_1}{30} \qquad D_3 = \frac{M_1 + M_2}{EAL^2} \quad \textbf{(3-30)}$$

If L is set equal to L_0 in Equations 3-27 and 3-28 then $\hat{k}_E$ and $\hat{k}_{G1}$ become the elastic and geometric stiffness matrices commonly found in the literature (ex. Yang et. al. 2002, Zhao et. al. 2006). The third matrix, $\hat{k}_{G2}$, is a higher-order local member geometric stiffness matrix. Note that $\hat{k}_{G2}$ is not symmetric. This is because the axial force does not take into account the lengthening of the curved shape in Figures 3-1 and 3-2 due to the end rotations, θ_1 and θ_2. A cubic polynomial is used to approximate the deformed shape of the member due to the end rotations in order to calculate the following expression for the axial force

$$F = \frac{EA}{L_0}(L - L_0) + EA\left(\frac{1}{15}\theta_1^{\,2} - \frac{1}{30}\theta_1\theta_2 + \frac{1}{15}\theta_2^{\,2}\right) \quad \textbf{(3-31)}$$

The derivation of the Equation 3-31 is given in Appendix A. The new equation for the axial force is used to obtain the following symmetric $\hat{k}_{G2}$ matrix

$$\hat{k}_{G2} = EA\begin{bmatrix} 0 & D_3 - \frac{D_1 + D_2}{L} & -D_1 & 0 & -D_3 + \frac{D_1 + D_2}{L} & -D_2 \\ D_3 - \frac{D_1 + D_2}{L} & \frac{L_0(D_1 + D_2)^2}{L^2} & \frac{L_0 D_1(D_1 + D_2)}{L} & -D_3 + \frac{D_1 + D_2}{L} & -\frac{L_0(D_1 + D_2)^2}{L^2} & \frac{L_0 D_2(D_1 + D_2)}{L} \\ -D_1 & \frac{L_0 D_1(D_1 + D_2)}{L} & L_0 D_1^2 & D_1 & -\frac{L_0 D_1(D_1 + D_2)}{L} & L_0 D_1 D_2 \\ 0 & -D_3 + \frac{D_1 + D_2}{L} & D_1 & 0 & D_3 - \frac{D_1 + D_2}{L} & D_1 \\ -D_3 + \frac{D_1 + D_2}{L} & -\frac{L_0(D_1 + D_2)^2}{L^2} & -\frac{L_0 D_1(D_1 + D_2)}{L} & D_3 - \frac{D_1 + D_2}{L} & \frac{L_0(D_1 + D_2)^2}{L^2} & -\frac{L_0 D_2(D_1 + D_2)}{L} \\ -D_2 & \frac{L_0 D_2(D_1 + D_2)}{L} & L_0 D_1 D_2 & D_1 & -\frac{L_0 D_2(D_1 + D_2)}{L} & L_0 D_2^2 \end{bmatrix} \quad \textbf{(3-32)}$$

4 Numerical Examples

4.1 Example: Cantilever Column

Consider the cantilever column shown in Figure 4-1, where L = 240 inches, P = 400 kips and Q = 50 kips. A large vertical load was chosen in order to assure that the p-delta effects were significant. The column has a modulus of elasticity equal to 29,000 ksi, a cross-sectional area equal to 100 in^2, and a moment of inertia of 833.3 in^4.

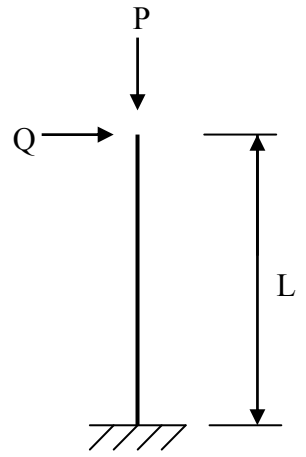

Figure 4-1 Cantilever Column

The cantilever column was analyzed using the method presented in this thesis, which incorporates the elastic, geometric and higher-order geometric stiffness matrices in the tangent stiffness matrix. The analysis yielded end displacements at the top of the column of 15.3 inches horizontally, 0.62 inches vertically downward and a rotation of 0.098 radians.

4.1.1 Comparison with ABAQUS/CAE

The same cantilever column example was modeled using the finite element software ABAQUS/CAE for comparison. The column was first analyzed using only one element. It was then divided into 200 elements and a second analysis was performed. The beam element B21 was used for both ABAQUS analyses, which is explained in Appendix B. Table 4-1 shows the results of this comparison. The ABAQUS analysis which used 200 elements was considered to be the most accurate of the three methods used to analyze this example. The errors between the results from the ABAQUS analysis with 200 elements and the other two analyses are shown in Table 4-2.

Table 4-1 Results of Three Analyses

Displacement	Present Method	ABAQUS/CAE with 1 element per member	ABAQUS/CAE with 200 elements per member
Horizontal (in)	15.344922	12.7932	15.3914
Vertical (in)	-0.624892	-0.374151	-0.631485
Rotation (rad)	-0.097584	-0.0848857	-0.0977828

Table 4-2 Comparison to the 200 Element ABAQUS Analysis

Displacement	Present Method	ABAQUS/CAE with 1 element per member
Horizontal (in)	0.3%	16.9%
Vertical (in)	1.0%	40.8%
Rotation (rad)	0.2%	13.2%

The analysis method presented in this thesis which used a single element to model the cantilever column and the ABAQUS model which used 200 elements yielded very similar results, with a maximum error of 1.0%. The ABAQUS analysis which used only one element to model the column had an error of 16.9% for the horizontal displacement and a maximum error of 40.8%.

A convergence study was done to determine the number of elements required for ABAQUS to obtain results with the same accuracy as the results from the analysis which used the element presented in this thesis. Figure 4-2 plots the horizontal displacement calculated by ABAQUS as a function of the number of elements used to analyze the column. Ten elements were required for the ABAQUS analysis to produce a similar horizontal displacement as the method presented in this thesis. The convergence study also verified the assumption that the ABAQUS analysis with 200 elements was accurate.

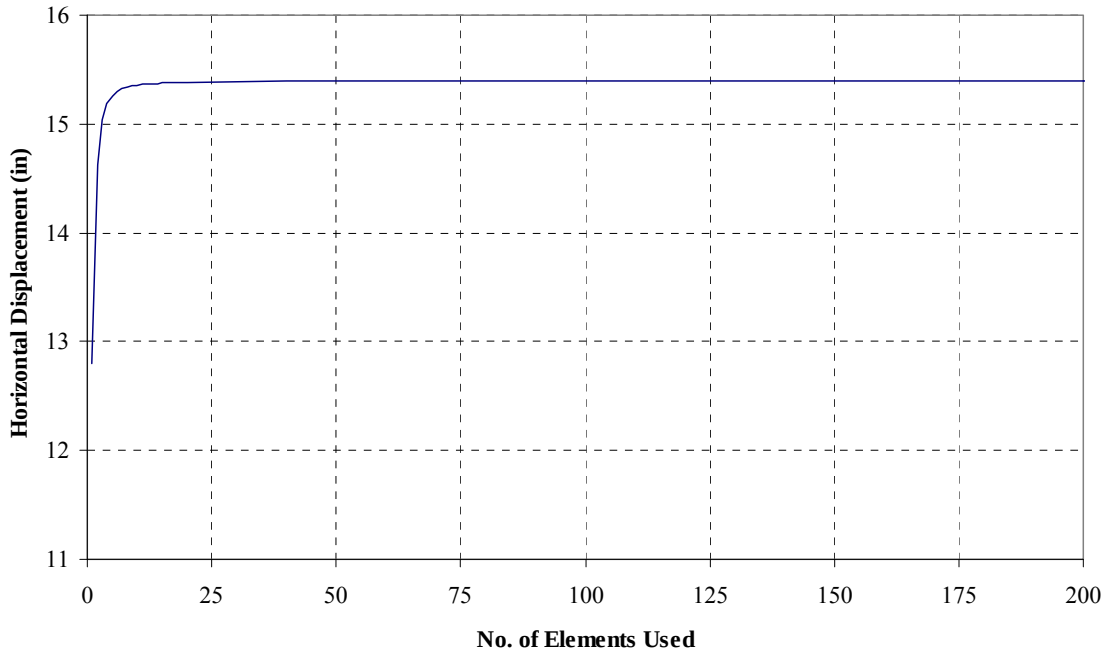

Figure 4-2 Convergence Study of ABAQUS Analysis

4.1.2 Validation of the Derivation of the Local Member Tangent Stiffness Matrix

The cantilever column example was also used to validate the derivation of the tangent stiffness matrix presented in section 3. An initial displacement vector was input into the analysis and the corresponding structure resistance vector was calculated. The following initial displacement vector was used

$$u = \begin{bmatrix} 1 & 1 & 1 \end{bmatrix}^{\mathrm{T}} \tag{4-1}$$

where displacements are measured in inches and rotations are measured in radians. Using the finite difference method the derivative of the resistance vector was determined and compared to the original tangent stiffness matrix. The structure tangent stiffness matrix that corresponds to the displacement vector in Equation 4-1 is

$$K_{\mathrm{T}} = \begin{bmatrix} 1180.3276 & 1161.9492 & 63641.1123 \\ 1161.9492 & 12073.878 & 387609.247 \\ 63641.112 & 387609.25 & 19466044.3 \end{bmatrix} \tag{4-2}$$

The structure tangent stiffness matrix computed using the finite difference method is

$$K_{\mathrm{T}} = \begin{bmatrix} 1180.33 & 1161.95 & 63646.99 \\ 1161.95 & 12073.88 & 387628.56 \\ 63641.22 & 387609.25 & 19467906.1 \end{bmatrix} \tag{4-3}$$

which constitutes a maximum error of 0.0096%. Such a small error suggests that the stiffness matrix calculated in the analysis is a reasonable approximation to the true derivative of the resistance vector.

4.1.3 Contributions of Sub-Matrices to the Tangent Stiffness Matrix

Equation 3-26 shows that the local member tangent stiffness matrix is the sum of three sub-matrices; $\hat{k}_E$=the elastic, $\hat{k}_{G1}$=geometric and $\hat{k}_{G2}$=higher-order geometric stiffness matrices. Figures 4-3, 4-4, and 4-5 show the contributions of these three sub-matrices to the local member tangent stiffness matrix in the first Newton-Raphson iteration as a function of the horizontal displacement, vertical displacement, and rotation, respectively. The contribution percentages were calculated element by element and then averaged over all the elements in the matrix.

Figure 4-6 shows the contribution percentages of the three sub-matrices to the local member tangent stiffness matrix as the horizontal and rotational displacements are simultaneously increased. The vertical displacement was set equal to zero. The following ratio was used to determine the rotation

$$\frac{\theta}{\Delta} = \frac{3}{2L} \qquad \textbf{(4-4)}$$

where Δ is the horizontal displacement and L is the height of the column. Equation 4-4 is the same equation used in first-order linear analysis to find the rotation at the end of a cantilever beam.

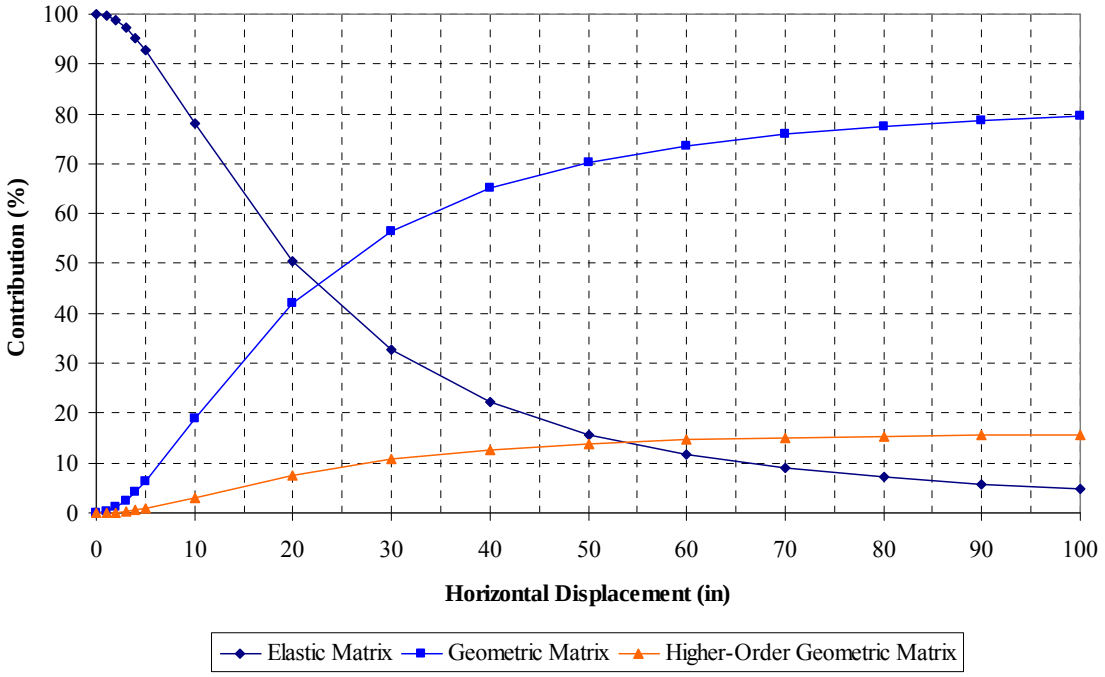

Figure 4-3 Contribution Percentages for Variable Horizontal Displacement

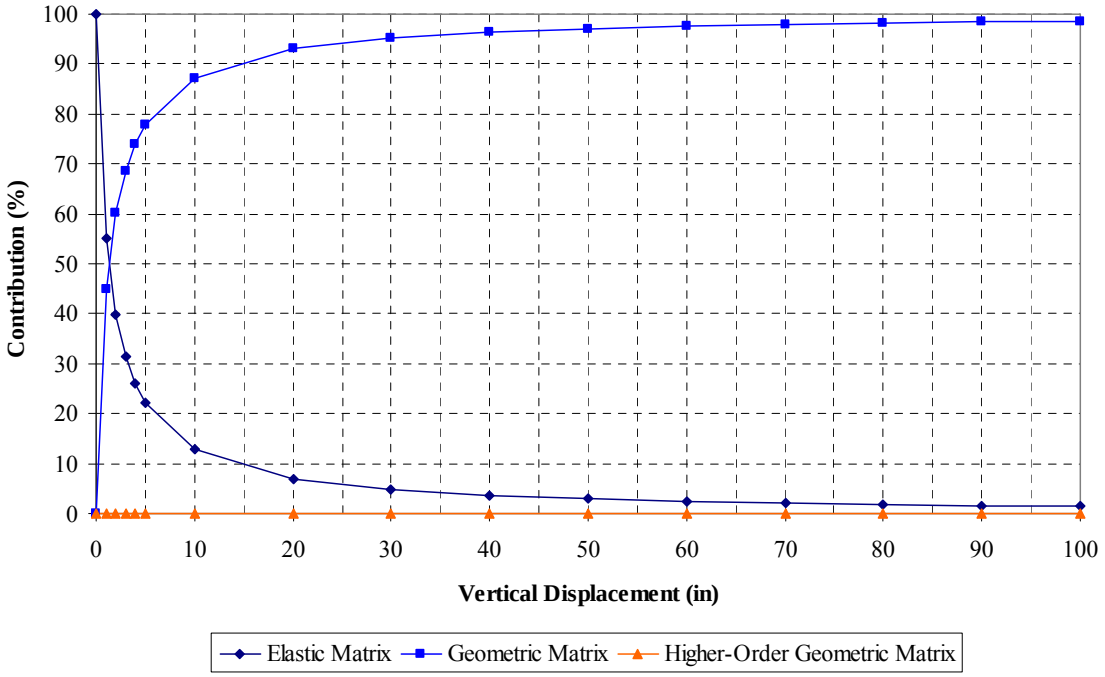

Figure 4-4 Contribution Percentages for Variable Vertical Displacement

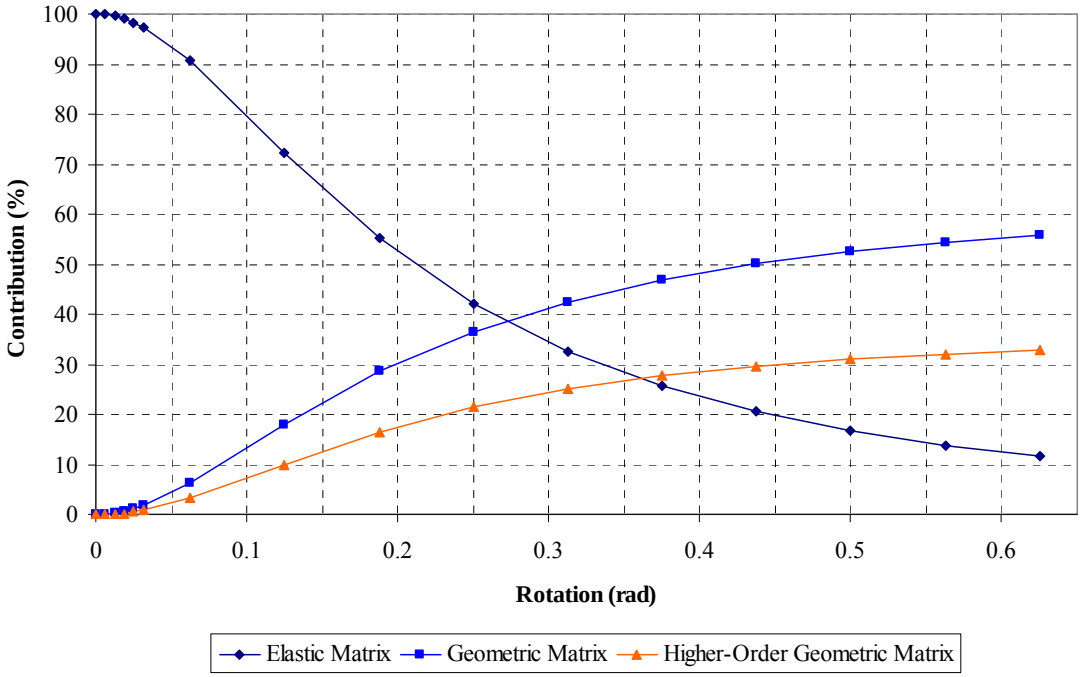

Figure 4-5 Contribution Percentages for Variable Rotation

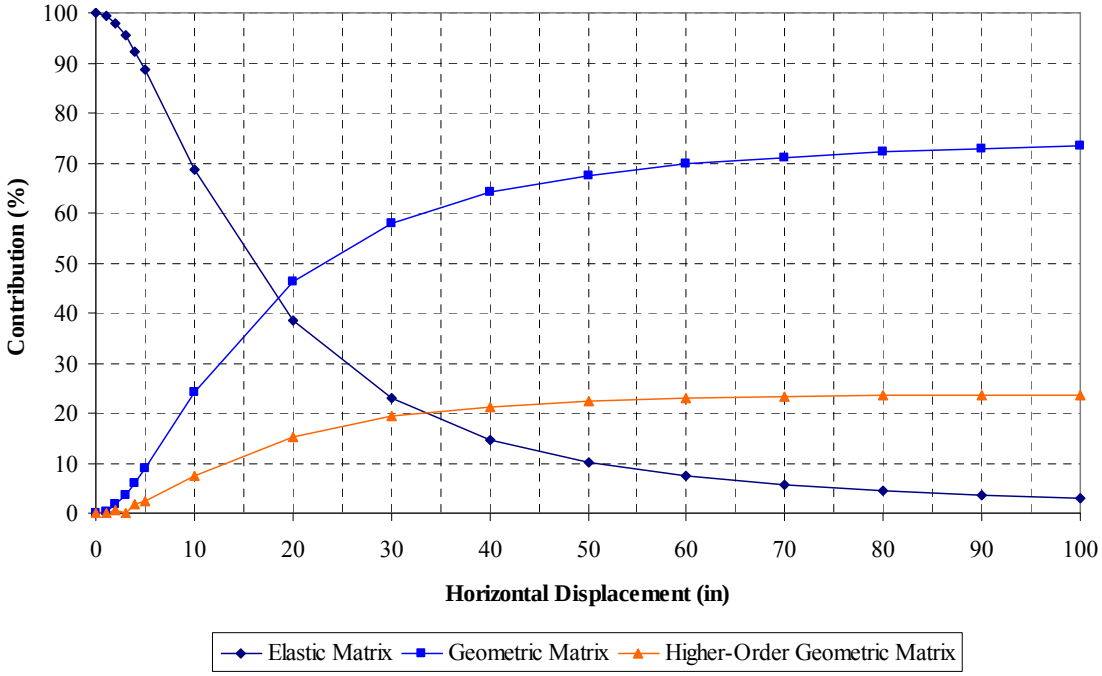

Figure 4-6 Contribution Percentages for Variable Displacements and Rotations

Figures 4-3 through 4-6 show that the elastic stiffness matrix constitutes most of the element's response when the displacements are small. The contributions of the geometric stiffness matrices increase as the deformations become larger. Figure 4-4 shows that the contribution of the higher-order geometric stiffness matrix is not affected by the vertical displacement.

The same procedure was used to obtain Figure 4-6, which shows the contributions of the sub-matrices to the structure tangent stiffness matrix. The horizontal and rotational displacements were increased simultaneously using Equation 4-4. The vertical displacement was set to zero. As Figure 4-7 demonstrates, the contributions from the geometric stiffness matrices to the structure tangent stiffness matrix increase as the deformations become larger.

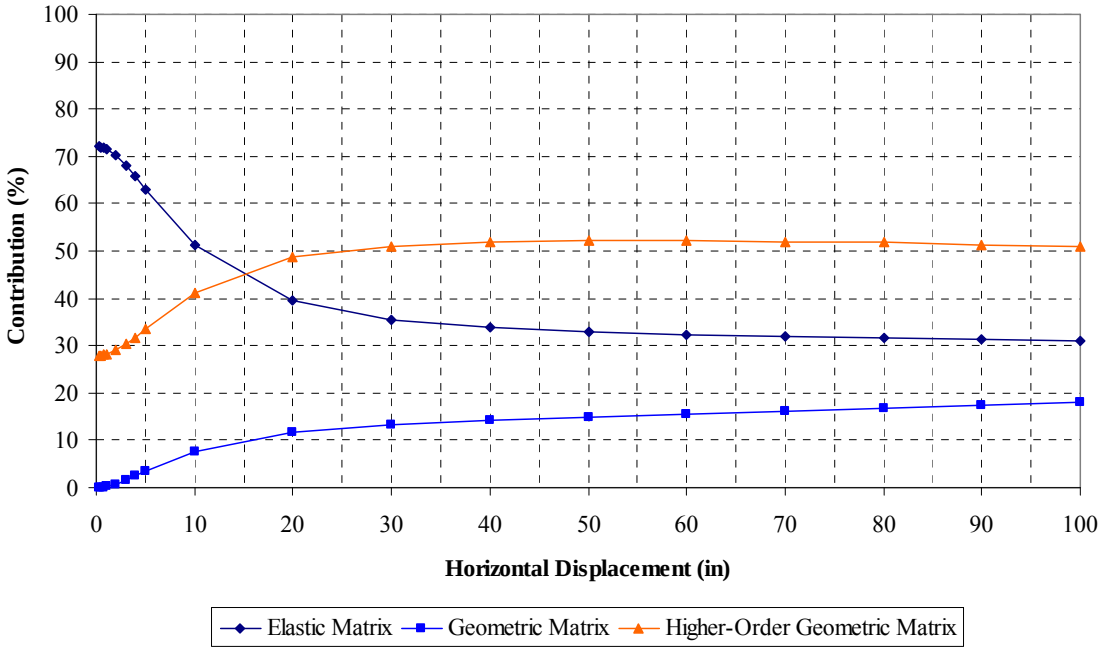

Figure 4-7 Contribution Percentages to the Structure Tangent Stiffness Matrix

4.2 Example: Two-Story Plane Frame

Consider the two-story plane frame shown in Figure 4-8, where L_1 = 120 inches and L_2=144 inches. The forces, P = 400 kips and Q = 50 kips are applied to joints 3 through 6. The letter J with a subscript is used to label the joints.

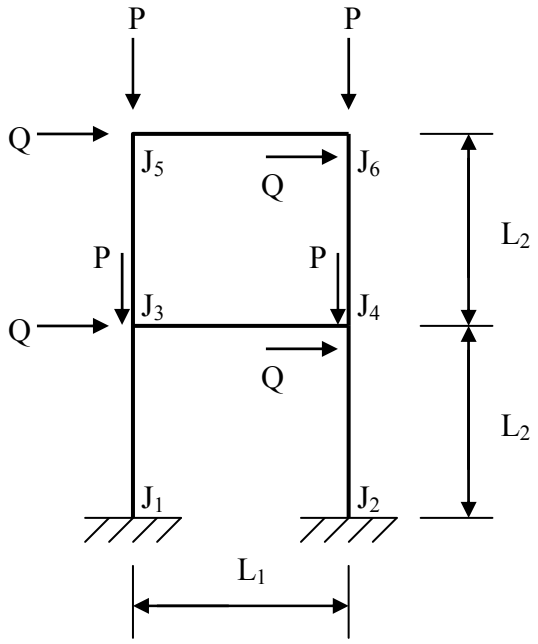

Figure 4-8 Two-Story Plane Frame

The columns have a cross-sectional area equal to 100 in^2, and a moment of inertia of 833.3 in^4. The girders have a cross-sectional area equal to 25 in^2, and a moment of inertia of 52.1 in^4. All of the members have a modulus of elasticity equal to 29,000 ksi.

An analysis was performed which incorporated the elastic, geometric and higher-order geometric stiffness matrices into the tangent stiffness matrix. The resulting joint displacements of the analysis are shown in Table 4-3.

Table 4-3 Displacements from the Analysis on the Two-Story Plane Frame

Joint	Horizontal Displacement (IN)	Vertical Displacement (IN)	Rotation (rad)
J_1	0.0	0.0	0.0
J_2	0.0	0.0	0.0
J_3	6.317	-0.199	-0.06800
J_4	6.263	-0.213	-0.06787
J_5	17.105	-0.619	-0.07054
J_6	17.047	-0.642	-0.07057

4.2.1 Comparison with ABAQUS/CAE

As was done with the cantilever column example, this same problem was modeled using the finite element software ABAQUS/CAE for comparison. Table 4-4 shows the results of the ABAQUS analysis which used only a single element per member. Table 4-5 shows the results of the ABAQUS analysis which used 200 elements per member. Once again, both ABAQUS analyses were done using the B21 element explained in Appendix B.

Table 4-4 Results from the ABAQUS Analysis with a Single Element per Member

Joint	Horizontal Displacement (IN)	Vertical Displacement (IN)	Rotation (rad)
J_1	0.0	0.0	0.0
J_2	0.0	0.0	0.0
J_3	4.927	-0.115	-0.05427
J_4	4.926	-0.133	-0.05427
J_5	13.315	-0.375	-0.05416
J_6	13.315	-0.401	-0.05417

Table 4-5 Results from the ABAQUS Analysis with 200 Elements per Member

Joint	Horizontal Displacement (IN)	Vertical Displacement (IN)	Rotation (rad)
J_1	0.0	0.0	0.0
J_2	0.0	0.0	0.0
J_3	6.362	-0.201	-0.06831
J_4	6.308	-0.216	-0.06818
J_5	17.215	-0.627	-0.07094
J_6	17.156	-0.650	-0.07096

The comparison of the analysis using the method presented in this thesis and the ABAQUS analysis which used 200 elements per member is given in Table 4-6. The comparison between the ABAQUS analysis which used a single element per member and the ABAQUS analysis which used 200 elements per member is given in Table 4-7.

Table 4-6 Error between the Present Analysis and the 200 Element per Member ABAQUS Analysis

Joint	Horizontal Displacement	Vertical Displacement	Rotation
J_3	0.7%	1.4%	0.5%
J_4	0.7%	1.4%	0.5%
J_5	0.6%	1.2%	0.6%
J_6	0.6%	1.2%	0.5%

Table 4-7 Error between the Two ABAQUS Analyses

Joint	Horizontal Displacement	Vertical Displacement	Rotation
J_3	22.6%	42.8%	20.6%
J_4	21.9%	38.7%	20.4%
J_5	22.7%	40.2%	23.6%
J_6	22.4%	38.3%	23.7%

The analysis using the method presented in this thesis and the ABAQUS analysis which used 200 elements per member yielded very similar results, with a maximum error of 1.4%. Once again, the method presented in this thesis gave reasonable results with the use of only one element per member. The maximum errors between the two ABAQUS analyses were 22.7% for the horizontal displacements and 42.8% for the vertical displacements.

4.2.2 Contributions of the Sub-Matrix to the Tangent Stiffness Matrix

Figure 4-9 plots the contributions of the three sub-matrices to the structure tangent stiffness matrix for the two-story plane frame example. The same procedure was used to generate Figure 4-9 as was used in the cantilever column example. The relative horizontal displacements and the rotations were incremented simultaneously for each story using the relationship given in Equation 4-4. The vertical displacements were set to zero.

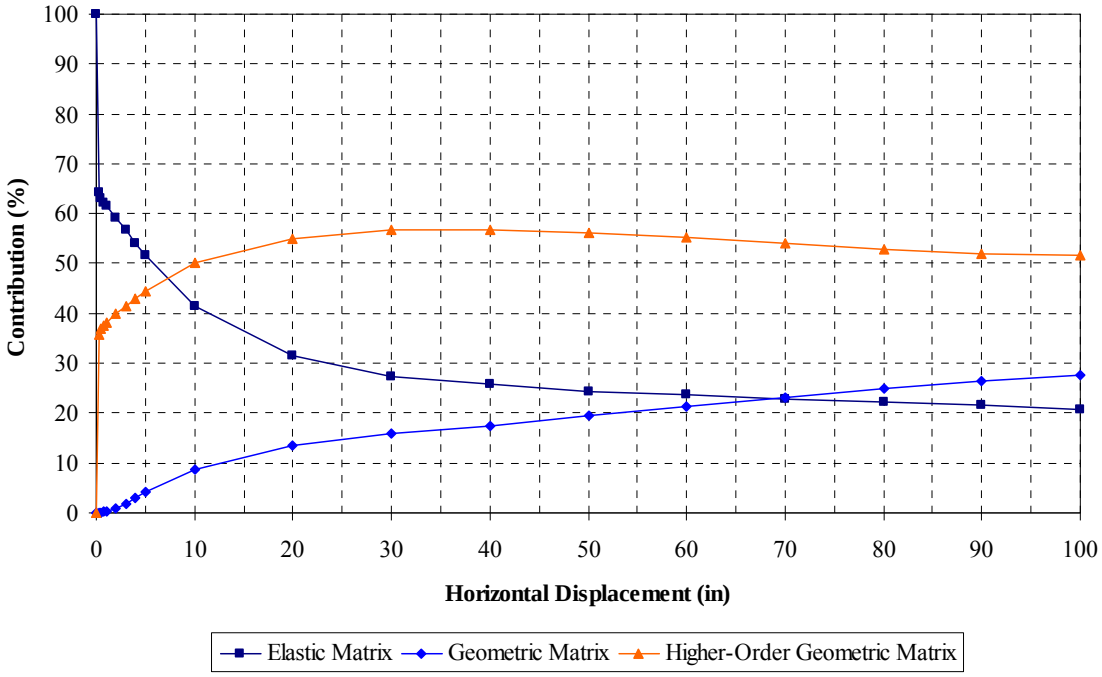

Figure 4-9 Contributions to the Structure Tangent Stiffness Matrix

Figure 4-9 shows that the elastic stiffness matrix constitutes most of the structure's response when the displacements are small. The two geometric stiffness matrices become more important in the analysis as the deformations become larger.

5 Conclusions

The first objective of this thesis was to present a second-order nonlinear plane frame analysis method which uses only one element per member. The second objective was to derive a tangent stiffness matrix for the plane frame element that is the direct derivative of the resistance vector. Both objectives have been achieved. Formulas for the local tangent stiffness matrix have been successfully derived by differentiating the member resistance vector in the displaced position which facilitates an analysis using only one element per member. These formulas have been checked by finite difference. The derivation led to the familiar elastic and geometric stiffness matrices used by other authors with an additional higher order geometric stiffness matrix.

Contributions of each of the sub-matrices to the tangent stiffness matrix were studied on both the member and structure levels through two numerical examples. At small deformations, the elastic stiffness matrix contributed the most to the tangent stiffness matrix. The contributions from the geometric stiffness matrices increased as the displacements became larger.

A cantilever column example and a two-story plane frame example were analyzed three different ways for comparison. First, each example was analyzed using the method presented in this thesis. Second, each example was analyzed with the finite element modeling software ABAQUS/CAE using only one element per member. A third analysis

was performed using ABAQUS/CAE with 200 elements per member. The ABAQUS analysis which used 200 elements per member was assumed to be the most accurate. Comparisons were made between it and the other two analyses. The ABAQUS analysis which used one element per member had maximum errors of 41% for the cantilever column example and 43% for the two-story plane frame example. The element presented in this thesis performed much better, with maximum errors of only 1% for the cantilever column example and 1.4% for the two-story plane frame example.

There are, however, limitations to the application of this element in structural analysis. The derivation of the tangent stiffness matrix neglects the shear deformation of the members and assumes that the material remains elastic. Furthermore, this element only applies to plane frames and has not been extended to three-dimensional frames. Despite these limitations, using the element presented in this thesis with only one element per member gives good and computationally efficient results for second-order analysis.

References

Albermani, F. G. A., S. Kitipornchai. "Nonlinear-Analysis of Thin-Walled Structures Using Least Element Member." *Journal of Structural Engineering-ASCE,* 116(1) (Jan. 1990): 215-234.

Chan, S. L., Z. H. Zhou. "Second-Order Elastic Analysis of Frames Using Single Imperfect Element per Member." *Journal of Structural Engineering-ASCE*, 121(6) (Jun. 1995): 939-945.

Chandra, R., D. N. Trikha, P. Krishna. "Nonlinear analysis of steel space frames." *Journal of Structural Engineering-ASCE*, 116(4) (Apr. 1990): 898-909.

Cheney, W., D. Kincaid. *Numerical Mathmatics and Computing, Sixth edition*. Belmont, C.A.: Thomson Brooks/Cole, 2008.

"Choosing a beam element." *ABAQUS Analysis User's Manual, Version 6.8*. Providence, R.I.: Simulia, 2008.

Gu, J., S. Chan. "Exact tangent stiffness for imperfect beam-column members." *Journal of Structural Engineering*, 126 (Sep. 2000): 1094-1102.

Gu, J., S. Chan. "Tangent stiffness matrix for geometric nonlinear analysis of space frames." *Journal of Southeast University (English Addition)*, 21(4) (Dec. 2005): 480-485.

Haktanir, V. "New method for element stiffness matrix of arbitrary planar bars." *Computers and Structures*, 52(4) (Aug. 1994): 679-691.

Izzuddin, B. A. "Simplified buckling analysis of skeletal structures." *Proceedings of the Institute of Civil Engineers-Structures and Buildings*, 159(6) (Aug. 2006): 631-651.

Leu, L. J., J. P. Yang, M. H. Tsai, Y. B. Yang. "Explicit Inelastic Stiffness for Beam Elements with Uniform and Nonuniform Cross Sections." *Journal of Structural Engineering*, 134(4) (April 2008): 608-618.

Morán, A., E. Oñate, J. Miquel. "A General Procedure for Deriving Symmetric Expressions for the Secant and Tangent Stiffness Matrices in Finite Element Analysis." *International Journal for Numerical Methods Engineering,* 42 (1998): 219-236.

Oran, M. C. "Tangent Stiffness in Plane Frames." *Journal of Structural Division*, 99(6) (Jun. 1973a): 973-984.

Oran, M. C. "Tangent Stiffness in Space Frames." *Journal of Structural Division*, 99(6) (Jun. 1973b): 987-1001.

So, A. K. W., S. L. Chan. "Buckling and Geometrically Nonlinear Analysis of Frames using One Element/Member." *Journal of Construction Steel Research,* 20 (1991): 271-289.

Shoup, T. E., C. W. McLarnan. "On the use of the Undulating Elastica for the Analusis of Flexible Link Mechanisms." Journal of Engineering for Industry, 93(1) (Feb. 1971): 263-267.

Yang, Y. B., H. T. Chiou. "Rigid Body Motion Test for Nonlinear-Analysis with Beam Elements." *Journal of* Engineering *Mechanics – ASCE*, 113(9) (September 1987): 1404-1419.

Yang, Y. B., S. R. Kuo. *Theory and Analysis of Nonlinear Framed Structures.* Englewood Cliffs, N.J.: Prentice-Hall, 1994.

Yang, Y. B., S. R. Kuo, Y. S. Wu. "Incrementally small-deformation theory for nonlinear analysis of structural frames." *Engineering Structures*, 24(6) (2002): 783-798.

Yang, Y. B., S. P. Lin, C. M. Wang. "Rigid element approach for deriving the geometric stiffness of curved beams for use in buckling analysis." *Journal of Structural Engineering – ASCE,* 133(12) (Dec. 2007): 1762-1771.

Yang, Y.B., W. McGuire. "Stiffness Matrix for Geometric Nonlinear Analysis." *Journal of Structural Engineering – ASCE,* 112(4) (April 1986): 853-877.

Zielinski, A. P., F. Frey. "On linearization in nonlinear structural finite element analysis." *Computers & Science*, 79(8) (March 2001): 825-838.

Zhao, D. F., K. K. F. Wong. "New approach for seismic nonlinear analysis of inelastic framed structures." *Journal of Engineering Mechanics*, 132(9) (Sept. 2006): 959-966.

Zhou, Z. H., S. L. Chan. "Elastoplastic and Large Deflection Analysis of Steel Frames by One Element per Member. I: One Hinge Along Member." *Journal of Structural Engineering – ASCE,* 130(4) (Apr. 2004a): 538-544.

Zhou, Z. H., S. L. Chan. "Elastoplastic and Large Deflection Analysis of Steel Frames by One Element per Member. II: Three Hinges Along Member." *Journal of Structural Engineering – ASCE,* 130(4) (Apr. 2004b): 545-553.

Appendix A Member End Moments and Axial Force

A.1 Derivation of the Member End Moments

The present derivation is used to determine the end moments of a plane frame member given in Equation 3-2. Before beginning with the derivation, the governing equation of second-order Euler theory must be derived. Consider the infinitesimal section of a plane frame member in its deformed configuration as shown in Figure A-1.

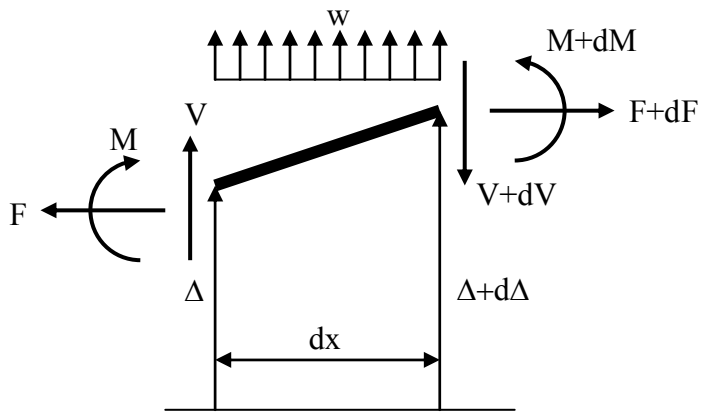

Figure A-1 An Infinitesimal Section of a Plane Frame Member

The displacements from the original position are Δ and Δ+dΔ at the left and right ends, respectively. Setting the sum of the horizontal forces equal to zero yields the following

$$F + dF - F = dF = 0 \quad \textbf{(A-1)}$$

By setting the summation of the vertical forces equal to zero, the following is determined

$$V + wdx - V - dV = wdx - dV = 0 \quad \textbf{(A-2)}$$

A third equation is developed by setting the sum of the moments about the right end equal to zero.

$$M + dM - M - Vdx - F(\Delta + d\Delta - \Delta) - wdx\frac{dx}{2}$$

$$= dM - Vdx - Fd\Delta - w\frac{dx^2}{2} = 0 \quad \textbf{(A-3)}$$

By dividing Equations A-1 through A-3 by *dx* the following three equations are obtained

$$\frac{dF}{dx} = 0 \quad \textbf{(A-4)}$$

$$w - \frac{dV}{dx} = 0 \quad \textbf{(A-5)}$$

$$\frac{dM}{dx} - V - F\frac{d\Delta}{dx} - w\frac{dx}{2} = 0 \quad \textbf{(A-6)}$$

In the limit as *dx* goes to zero Equation A-6 becomes

$$\frac{dM}{dx} - V - F\frac{d\Delta}{dx} = 0 \quad \textbf{(A-7)}$$

Differentiating Equation A-7 and substituting from Equations A-4 and A-5

$$\frac{d^2M}{dx^2} - F\frac{d^2\Delta}{dx^2} = w \qquad \textbf{(A-8)}$$

Substituting the flexural constitutive equation into Equation A-8

$$EI\frac{d^4\Delta}{dx^4} - F\frac{d^2\Delta}{dx^2} = w \qquad \textbf{(A-9)}$$

With Equation A-9, the governing equation of second-order Euler beam theory, the end moments of a plane frame member can be derived.

Consider the skeletal member shown in Figure A-2. This member may be part of a plane frame. The dotted line represents the deformed configuration of the member.

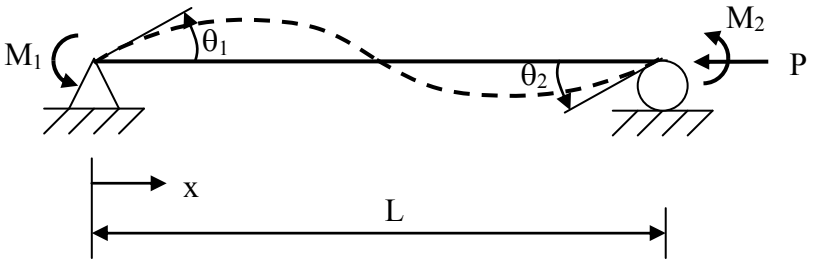

Figure A-2 A Plane Frame Member

The angles θ_1 and θ_2 are the end rotations at the left and right ends of the member, respectively. M_1 and M_2 are the end moments of the left and right ends of the member,

respectively. For this derivation, the uniform load along the beam, *w* is set to zero, and the axial force in the member is P. The governing differential equation becomes

$$EI\frac{d^4\Delta}{dx^4} - P\frac{d^2\Delta}{dx^2} = 0 \qquad \textbf{(A-10)}$$

The general solution to Equation A-10 is

$$\Delta(x) = a\sin\frac{\lambda x}{L} + b\cos\frac{\lambda x}{L} + cx + d \qquad \textbf{(A-11)}$$

where

$$\lambda = L\sqrt{\frac{P}{EI}}$$

By differentiating Equation A-11, the following equations for the rotation and bending moment are obtained

$$\theta(x) = \frac{d\Delta}{dx} = \frac{a\lambda}{L}\cos\frac{\lambda x}{L} - \frac{b\lambda}{L}\sin\frac{\lambda x}{L} + c \qquad \textbf{(A-12)}$$

$$M(x) = EI\frac{d^2\Delta}{dx^2} = -EI\frac{\lambda^2}{L^2}\left(a\sin\frac{\lambda x}{L} + b\cos\frac{\lambda x}{L}\right) \qquad \textbf{(A-13)}$$

Applying the appropriate boundary conditions to Equations A-11 through A-13, equations for the coefficients a and b are determined.

$$\begin{Bmatrix} a \\ b \end{Bmatrix} = \frac{L}{\lambda(2 - 2\cos\lambda - \lambda\sin\lambda)}\begin{bmatrix} 1-\cos\lambda-\lambda\sin\lambda & \cos\lambda - 1 \\ \sin\lambda - \lambda\cos\lambda & \lambda - \sin\lambda \end{bmatrix}\begin{Bmatrix} \theta_1 \\ \theta_2 \end{Bmatrix} \qquad \textbf{(A-14)}$$

The coefficients c and d can then be calculated using the values of a and b.

$$c = -\frac{a}{L}\sin\lambda + \frac{b}{L}\left(1-\cos\lambda\right)\right) \tag{A-15}$$

$$d = -b \tag{A-16}$$

To obtain equations for the end moments of the member, two addition boundary conditions are used.

At x = 0, M = M_1:

$$-EI\frac{\lambda^2}{L^2}b = -M_1 \tag{A-17}$$

At x = L, M = M_2:

$$-EI\frac{\lambda^2}{L^2}\left(a\sin\lambda + b\cos\lambda\right) = M_2 \tag{A-18}$$

Equations A-17 and A-18 can be written in matrix form as follows

$$\begin{Bmatrix} M_1 \\ M_2 \end{Bmatrix} = EI\frac{\lambda^2}{L^2}\begin{bmatrix} 0 & 1 \\ -\sin\lambda & -\cos\lambda \end{bmatrix}\begin{Bmatrix} a \\ b \end{Bmatrix} \tag{A-19}$$

Substituting a and b into Equation A-19

$$\begin{Bmatrix} M_1 \\ M_2 \end{Bmatrix} = \frac{EI\lambda}{L\left(2-2\cos\lambda-\lambda\sin\lambda\right)}\begin{bmatrix} \sin\lambda-\lambda\cos\lambda & \lambda-\sin\lambda \\ \lambda-\sin\lambda & \sin\lambda-\lambda\cos\lambda \end{bmatrix}\begin{Bmatrix} \theta_1 \\ \theta_2 \end{Bmatrix} \tag{A-20}$$

The above derivation is valid for an axial force, P of tension. A similar process can be used to derive the end moments of a plane frame member where P is a compression force. Equation A-21 is the result of such a derivation.

$$\begin{Bmatrix} M_1 \\ M_2 \end{Bmatrix} = \frac{EI\lambda}{L(2-2\cosh\lambda+\lambda\sinh\lambda)} \begin{bmatrix} \lambda\cosh\lambda-\sinh\lambda & \sinh\lambda-\lambda \\ \sinh\lambda-\lambda & \lambda\cosh\lambda-\sinh\lambda \end{bmatrix} \begin{Bmatrix} \theta_1 \\ \theta_2 \end{Bmatrix} \quad \textbf{(A-21)}$$

where

$$\lambda = L\sqrt{\frac{P}{EI}}$$

A.2 Derivation of the Axial Force

The derivation of the axial force in a plane frame member given in Equation 3-31 follows. The axial force in a member is equal to the cross sectional area of that member multiplied by the stress applied to the cross section. This is represented in Equation A-22.

$$F = \frac{EA}{L_0}(L - L_0) \quad \textbf{(A-22)}$$

where

L = the length of the member in the deformed position

L_0 = the length of the member in the original position

E = the modulus of elasticity of the member

A = the cross sectional area of the member

The axial force presented in Equation A-22 leads to an asymmetric higher-order geometric stiffness matrix, because it does not take into to account the lengthening of the member due to the end rotations.

In order to determine the lengthening due to the end rotations, consider the skeletal member shown in Figure A-3. This member may be part of a plane frame. The solid line shows the undeformed position of the member, while the dotted line represents the deformed configuration of the member.

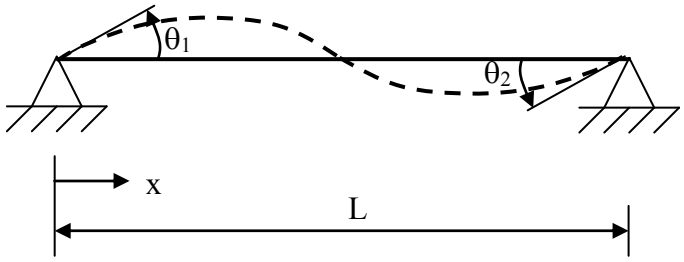

Figure A-3 A Plane Frame Member

The angles θ_1 and θ_2 are the end rotations at the left and right ends of the member, respectively. Notice that L in this figure refers to the length of the member in its undeformed position. To begin, the deformed shape is approximated by a cubic polynomial.

$$\Delta = ax^3 + bx^2 + cx + d \qquad \textbf{(A-23)}$$

The slope of the deformed member is

$$\theta = 3ax^2 + 2bx + c \qquad \textbf{(A-24)}$$

By using the correct boundary conditions the coefficients a, b, c and d are determined. The following four equations constitute Equation A-25.

$$a = \frac{\theta_1 + \theta_2}{L^2}$$
$$b = -\frac{2\theta_1 + \theta_2}{L} \qquad \textbf{(A-25)}$$
$$c = \theta_1$$
$$d = 0$$

The deformed length of the member is

$$\int_0^L \sqrt{1 + \left(\frac{d\Delta}{dx}\right)^2}\, dx = \int_0^L \sqrt{1 + \theta^2}\, dx \qquad \textbf{(A-26)}$$

Using the following first-order Maclaurin series approximation,

$$\sqrt{1+y} \approx 1 + \frac{y}{2}$$

Equation A-26 becomes

$$\int_0^L \left(1 + \frac{\theta^2}{2}\right) dx$$
$$= \int_0^L \left(1 + \frac{9a^2b^4}{2} + 6abx^3 + 3acx^2 + 2b^2x^2 + 2bcx + \frac{c^2}{2}\right) dx$$
$$= L + \frac{9a^2b^5}{10} + \frac{3abL^3}{2} + acL^3 + \frac{2b^2L^3}{3} + bcL^2 + \frac{c^2L}{2} \qquad \textbf{(A-27)}$$

Then substituting from Equation A-25, Equation A-27 becomes

$$L\left(\begin{array}{l}1+\dfrac{9(\theta_1+\theta_2)^2}{10}-\dfrac{3(\theta_1+\theta_2)(2\theta_1+\theta_2)}{2}+(\theta_1+\theta_2)\theta_1\\+\dfrac{2(2\theta_1+\theta_2)^2}{3}-(2\theta_1+\theta_2)\theta_1+\dfrac{\theta_1^{\,2}}{2}\end{array}\right)$$

$$=L\left(1+\frac{\theta_1^{\,2}}{15}-\frac{\theta_1\theta_2}{30}+\frac{\theta_2^{\,2}}{15}\right) \qquad \textbf{(A-28)}$$

The strain is equal to the change in length over the original length. By subtracting L from Equation A-28 and then dividing by L, the following strain is found

$$\frac{\theta_1^{\,2}}{15}-\frac{\theta_1\theta_2}{30}+\frac{\theta_2^{\,2}}{15} \qquad \textbf{(A-29)}$$

The axial force in the member is determined by multiplying the strain by the modulus of elasticity, E, to get the stress and then multiplying the stress by the cross sectional area, as follows

$$F=EA\left(\frac{\theta_1^{\,2}}{15}-\frac{\theta_1\theta_2}{30}+\frac{\theta_2^{\,2}}{15}\right) \qquad \textbf{(A-30)}$$

Equation A-30 is added to Equation A-22 to get the total axial force in the member.

$$F=\frac{EA}{L_0}(L-L_0)+EA\left(\frac{\theta_1^{\,2}}{15}-\frac{\theta_1\theta_2}{30}+\frac{\theta_2^{\,2}}{15}\right) \qquad \textbf{(A-31)}$$

Using the axial force given in Equation A-31, the derivation of the higher-order geometric stiffness matrix leads to the symmetric matrix in Equation 3-32.

Appendix B ABAQUS Element B21

The B21 element was used in all of the ABAQUS analyses presented in this thesis. The following comes from the information found in the "Choosing a beam element" section of the *ABAQUS Analysis User's Manual*. According to the naming convention used by ABAQUS, the B21 element is a two-dimensional beam element that uses a linear interpolation formulation. It can be used for slender beams as well as for non-slender or deep beams. The user may specify whether shear deformation of the beam is considered.